Development of a spinal locomotor rheostat

Hong-Yan Zhang, Jon Issberner[1], and Keith T. Sillar[2]

School of Biology, University of St Andrews, St Andrews, Fife KY16 9TS, Scotland, United Kingdom

Edited* by Sten Grillner, Karolinska Institutet, Stockholm, Sweden, and approved June 6, 2011 (received for review December 9, 2010)

Locomotion in immature animals is often inflexible, but gradually acquires versatility to enable animals to maneuver efficiently through their environment. Locomotor activity in adults is produced by complex spinal cord networks that develop from simpler precursors. How does complexity and plasticity emerge during development to bestow flexibility upon motor behavior? And how does this complexity map onto the peripheral innervation fields of motorneurons during development? We show in postembryonic *Xenopus laevis* frog tadpoles that swim motorneurons initially form a homogenous pool discharging single action potential per swim cycle and innervating most of the dorsoventral extent of the swimming muscles. However, during early larval life, in the prelude to a free-swimming existence, the innervation fields of motorneurons become restricted to a more limited sector of each muscle block, with individual motorneurons reaching predominantly ventral, medial, or dorsal regions. Larval motorneurons then can also discharge multiple action potentials in each cycle of swimming and differentiate in terms of their firing reliability during swimming into relatively high-, medium-, or low-probability members. Many motorneurons fall silent during swimming but can be recruited with increasing locomotor frequency and intensity. Each region of the myotome is served by motorneurons spanning the full range of firing probabilities. This unfolding developmental plan, which occurs in the absence of movement, probably equips the organism with the neuronal substrate to bend, pitch, roll, and accelerate during swimming in ways that will be important for survival during the period of free-swimming larval life that ensues.

motor system | central pattern generator | ontogeny

Adult vertebrates navigate through their environment with incredible agility and flexibility, a feature of locomotory behavior that is often critical for survival. During locomotion, sensory information interacts with central pattern generator (CPG) networks in the spinal cord, which in turn provide command signals to motorneurons (MNs) to sequence and guide movements appropriately (1). CPGs develop before locomotion is possible (2–4). Initially, however, the output of immature CPGs lacks the precision and flexibility that typifies adult locomotion. Therefore, postembryonic development must involve a period during which the central motor control circuitry is modified to accommodate the behavioral requirements of later stages. Much is known about the molecular mechanisms responsible for the differentiation of neuronal components of the motor system, motor axon trajectories, and innervation patterns (5–7). However, how this links to the functional development of these components has not been fully resolved, although there is ample evidence that activity itself is influential as a developmental signal (8, 9).

Recent evidence has revealed a topographic recruitment order for dorsoventrally arranged spinal premotor interneurons and MNs during changes in swimming speed in larval zebrafish (10, 11). Ventrally located MNs are active at lower swimming frequencies whereas more dorsally positioned MNs are engaged at progressively higher swimming frequencies. However, it is not known how this recruitment order maps onto the peripheral innervation fields of MNs or how this complexity emerges during embryonic development to impart flexibility to locomotion. In the adult lamprey, MNs supplying the swimming muscles belong to one of two distinct spinal populations that possess different dendritic field organizations and innervate the dorsal or ventral regions of the segmented muscle blocks, respectively (12). The two populations display differences in the amplitude and phasing of the synaptic drive during NMDA-induced fictive swimming, suggesting asymmetrical descending inputs that may be related to the requirement for control in the dorsoventral plane during righting and steering responses.

Here we have studied the rapid development of spinal locomotor circuitry in *Xenopus laevis* frog tadpoles in which self-sustaining locomotor activity can be triggered in immobilized animals without the requirement for exogenous excitants. This system has already allowed a detailed description of the locomotor CPG (13). We have focused on how MNs change during the first day of postembryonic development, a period when the motor system is changing rapidly and acquiring the flexibility that will soon be required for efficient free-swimming larval life (3, 14). At the time of hatching (stage 37/38) (15), tadpole MNs form a relatively homogeneous pool, each normally discharging one action potential per locomotor cycle and innervating most of the dorsoventral extent of the myotome. By larval stage 42, approximately 1 day later, this relatively stereotyped embryonic organization has changed markedly. MNs have differentiated morphologically into those that supply predominantly dorsal, medial, or ventral regions of the muscle block. In parallel, the MNs have differentiated physiologically into units with different firing probabilities; units with relatively low firing probabilities often do not fire during swimming but can be recruited during increases in locomotor frequency and burst intensity. Each dorsoventral region of the myotome is also supplied by motorneurons across the range of firing probabilities within the motor pool. This rapid differentiation of the morphological and physiological properties of the motorneurons underpins the flexibility and variability in the motor pattern that is acquired during a brief period of postembryonic development. The changes that we describe provide a neuronal substrate from which different forms of locomotor speed and direction can be selected, akin to a rheostatic control device.

Results

Homogeneous Structure and Function of Embryonic MNs. *Xenopus* tadpoles near the time of hatching [stage 37/38 (15); Fig. 1 *A*, *i*] generate a rhythmic swimming motor pattern that can be recorded from spinal ventral roots (VRs) in immobilized animals (Fig. 1 *A*, *ii* and *B*, lower traces). During fictive swimming, MN activity at 10–20 Hz alternates across the spinal cord [left (L) versus right (R) VRs; Fig. 1 *A*, *ii*] and propagates rostro-caudally with a brief delay (dotted line, Fig. 1 *A*, *ii*). During an episode of swimming, ventral root burst amplitudes vary little (Fig. 1 *B*, *i*, lower trace), suggesting that the firing of individual MNs in each cycle is relatively constant and sustained (Fig. 1*B*, upper traces). To confirm earlier findings using sharp microelectrodes (16, 17)

Author contributions: H.-Y.Z. and K.S. designed research; H.-Y.Z., J.I., and K.S. performed research; H.-Y.Z. and K.S. analyzed data; and H.-Y.Z., J.I., and K.S. wrote the paper.

The authors declare no conflict of interest.

*This Direct Submission article had a prearranged editor.

[1]Present address: Medical and Biological Sciences Building, University of St Andrews, North Haugh, St Andrews, Fife KY16 9TF, United Kingdom.

[2]To whom correspondence should be addressed. E-mail: kts1@st-andrews.ac.uk.

www.pnas.org/cgi/doi/10.1073/pnas.1018512108

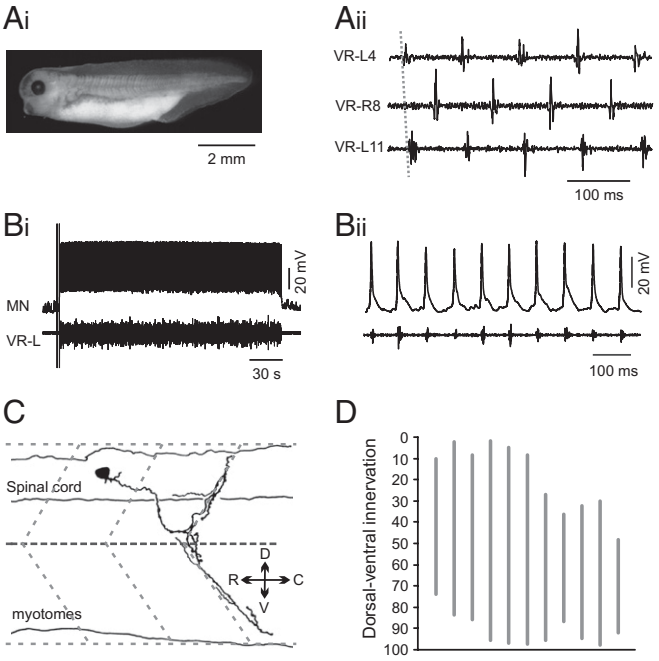

Fig. 1. Fictive swimming and MN morphology in *Xenopus* embryos. (*A*, *i*) Stage 37/38 embryo. (*A*, *ii*) Fictive swimming recorded from ventral roots (VR) at 4th and 11th clefts on the left side and 8th cleft on the right side of the embryo. Gray dotted line shows the rostrocaudal delay. (*B*, *i*) Whole-cell recording from MN on left side during entire swim episode and VR on left side (VR-L). (*B*, *ii*) Excerpt of activity to show single spike per cycle, in time with VR burst on same side as soma. Note reliable firing throughout episode. (*C*) Morphology of typical MN at stage 37/38 with soma in spinal cord and neurite exiting caudally before bifurcating and extending processes into the intermyotomal cleft. Overlay represents approximate positions of muscle blocks. Arrows indicate rostral (R), caudal (C), ventral (V), and dorsal (D). Convention applies to other anatomy figures. (*D*) Graph illustrating the dorsal to ventral extent of MN peripheral processes expressed as a percentage (dorsal = 0%; ventral = 100%).

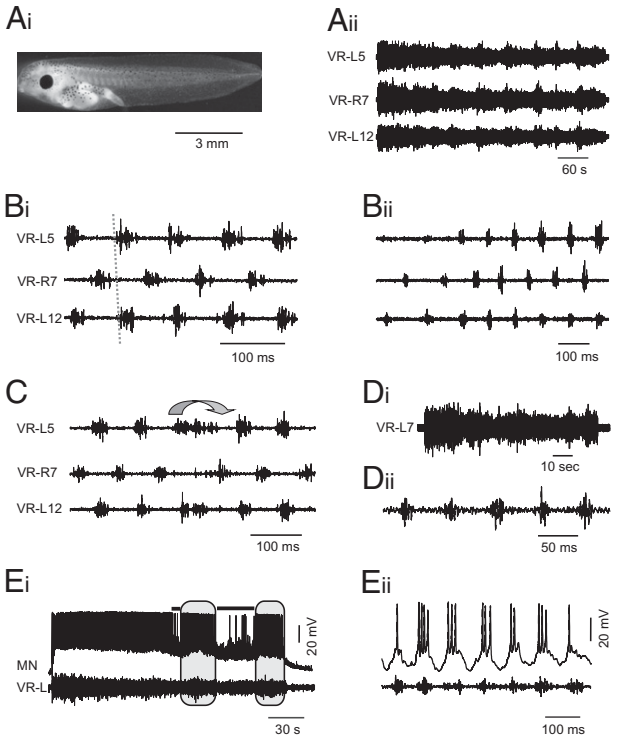

Fig. 2. Flexibility of larval swimming. (*A*, *i*) Stage 42 larva. (*A*, *ii*) Episode of fictive swimming (recorded as in Fig. 1 *B*, *i*) lasting several minutes. Note that VR amplitude waxes and wanes during the course of the episode. (*B*, *i*) Excerpt of activity. Note the similar coordination with left–right alternation and rostrocaudal delay (dotted gray line) but increased burst durations compared with stage 37/38. (*B*, *ii*) Spontaneous increase in cycle frequency and burst duration during fictive acceleration. (*C*) Fictive turning occurs spontaneously, involving increased activity on one side relative to the other; increased activity on left side (arrow) equals a fictive left turn. (*D*) Fictive swimming episode from stage 42 animal immobilized from stage 22 in MS222 reveals periodic waxing and waning of ventral root amplitudes (*D*, *i*) and longer burst durations (*D*, *ii*) typical of normal stage 42 activity (compare *D*, *i* with *A*, *ii* and *E*, *i* and compare *D*, *ii* with, e.g., *B*, *i*). (*E*) Patch recording from stage 42 MN; note that neuron fires multiple action potentials per cycle (*E*, *ii*) and falls silent during low-intensity activity (*E*, *i*, black bars), but can be recruited again when rhythm intensifies (gray boxes).

showing that stage 37/38 MNs normally fire once per cycle, irrespective of the swimming frequency, we made whole-cell patch clamp recordings ($n = 20$; Fig. 1*B*, upper traces) (18). The probability that a given MN will fire in each cycle is high and relatively constant during an episode (17).

The preparation used in the present study left the myotomal muscle blocks on the same side as the recorded neurons intact, enabling us to identify MNs unambiguously and to visualize their peripheral innervation patterns via inclusion of neurobiotin in the patch electrode (18). Shortly after exiting the spinal cord, the peripheral axon bifurcated to send branches to both dorsal and ventral aspects of each muscle block. Typically, stage 37/38 MNs had peripheral innervation fields that extended along the majority of the dorsoventral extent of the intermyotomal muscle cleft immediately caudal to the point of exit of the axon from the spinal cord (Fig. 1*C*; $n = 11$). The innervation field, as measured from the dorsal-most to the ventral-most labeled process, extended, on average, from 13.0% to 90.2%, thus covering 77.8% of the available myotome (Fig. 1 *C* and *D*). Several swellings were evident along the main peripheral processes, giving it a beaded appearance and presumably reflecting points of synaptic contact onto the ends of myotomal muscle fibers (19). There were relatively few short branches that projected laterally into the myotome, suggesting that the neuromuscular junctions are restricted mainly to the intermyotomal cleft regions.

Variability of the Larval Swimming Rhythm. Approximately 24 h later in development at larval stage 42 (Fig. 2 *A*, *i*) (15), fictive swimming activity (Fig. 2 *A*, *ii* and *B*) displays the same left–right and rostrocaudal coordination as at stage 37/38, but the brief biphasic ventral root bursts have been replaced by bursts of longer, more variable duration (14). This larval rhythm is overtly more variable than the embryonic one. Both the frequency and the intensity of ventral root bursts vary from cycle to cycle such that the rhythm waxes and wanes during the course of an episode with periods of high amplitude activity (Fig. 2 *A*, *ii* and *B*, *ii*) coinciding with high frequencies of swimming. Thus, activity can switch spontaneously from relatively slow and weak to fast and intense activity, and this can occur in the course of a few cycles during rapid accelerations (Fig. 2 *B*, *ii*). Furthermore, the intensity and duration of motor bursts can vary spontaneously between the left and right sides during fictive turning maneuvers when an increase in discharge is distributed along one side of the spinal cord with a corresponding delay to the next contralateral burst (Fig. 2*C*).

We next investigated whether the development of the more flexible larval rhythm is dependent on activity. Embryos were anesthetized in MS222 either from stage 22 (before the onset of any movement; $n = 8$) or from stage 37/38 ($n = 6$) until they reached stage 42. Development appeared to proceed normally, and experimental animals were indistinguishable from normal stage 42 animals. After removal from MS222 and immobilization

in α-bungarotoxin, recordings of fictive swimming were made; the rhythm displayed the main features of the normal larval rhythm with periodic variations in intensity (Fig. 2 *D*, *i*) and long burst durations (Fig. 2 *D*, *ii*).

The more variable and flexible features of the output of the larval swimming CPG presumably parallel significant changes in the myotomal motor pools to allow for the recruitment (or de-recruitment) of individual MNs during changes in the intensity or direction of swimming. To seek more direct evidence for this proposal, we made patch-clamp recordings from stage 42 MNs (n = 41). In contrast to stage 37/38 MNs (Fig. 1 *B*, *ii*), stage 42 MNs fired discrete bursts of action potentials in phase with the ipsilateral ventral root discharge (Fig. 2 *E*, *ii*), but often this activity fell below the spike threshold during lower-frequency swimming (Fig. 2 *E*, *i*; activity under black bars). This strongly indicates that by stage 42 the frequency and intensity of swimming activity correlates with the number of active MNs. In turn, this suggests that by early larval stages the CPG might now include MNs with a range of thresholds.

Development of Larval MN Innervation Fields. Larval MNs were also identified by neurobiotin injections and had axons projecting ventro-laterally from the spinal cord toward the ipsilateral myotome. In contrast to embryonic MNs, however, those labeled at stage 42 (n = 31 of 34) displayed more differentiated peripheral innervation fields that targeted a more restricted area of predominantly dorsal (Fig. 3 *A*, *i*), medial (Fig. 3 *A*, *ii*), or ventral (Fig. 3 *A*, *iii*) regions of the myotome. Although the innervation field of each larval MN was limited to a relatively narrow region, the MNs overlapped so that collectively they spanned the entire muscle block as a continuum from dorsal to ventral (Fig. 3*B*). Unlike their embryonic counterparts, stage 42 MNs often projected processes laterally into the myotome (e.g., Fig. 3 *A*, *ii*), suggesting that they make synaptic contact in areas of muscle beyond the intermyotomal cleft. These morphological changes suggest a rapid developmental reconfiguration of MNs from stage 37/38 in which new projections are extended and other processes retracted. The way in which the preparation was dissected precluded complete preservation of the central processes and cell bodies of MNs, making it difficult to investigate any correlation between the peripheral innervation field and the size or location of the MN somata or the extent of their dendritic fields. In a separate series of anatomical experiments, MNs were back-filled from muscles of intact preparations with rhodamine–dextran dyes (Fig. 3 *C*, *ii* and *iii*). In general, larval MNs were found in the same location of the spinal cord (Fig. 3*C*), but displayed more extensive dendritic arborisations (Fig. 3 *C*, *ii*) compared with stage 37/38 (19). The positions of the cell bodies were restricted to a relatively narrow ventro-medial band, but there was no correlation between soma size and position in the dorsoventral plane (Fig. 3 *C*, *i*; R^2 = 0.051). Furthermore, when the dorsally and ventrally innervating MNs were back-filled with different dyes (Fig. 3 *C*, *iii*), not only were two separate populations labeled, but also their cell body positions were intermingled. The total number of cell bodies labeled by back-filling was similar at stage 37/38 and stage 42, peaking at a maximum of 10–12/100 μm, indicating that the differences in innervation cannot be explained by the addition or deletion of MNs to the available pool.

Functional Development of Larval MNs. Larval MNs differ functionally from their embryonic precursors in their ability to fire multiply in each cycle and in that they may drop out during lower-frequency, lower-intensity swimming (Fig. 2 *E*, *i*). This suggests that the number of active MNs varies within an episode, with more MNs active during high-frequency, high-intensity activity. This leads to the hypothesis that a recruitment hierarchy exists with some MNs being recruited only during intense activity; in effect, the available motor pool must consist of units spanning a range of thresholds to allow the tadpole to vary its swimming activity in a manner akin to an electrical rheostat controlling, for example, a light dimmer.

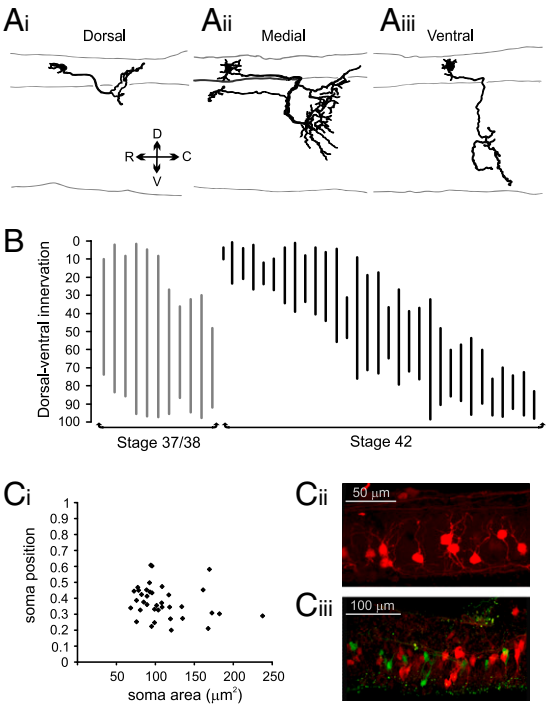

Fig. 3. Differentiation of larval MN anatomy and peripheral innervation fields. (*A*) Examples of MN morphology at stage 42 with innervation fields restricted mainly to different sectors of the myotome (*i*, dorsal; *ii*, medial; *iii*, ventral). Note the laterally projecting process in medial neuron in *A*, *ii*. (*B*) Innervation fields of 31 MNs; 11 innervated exclusively the dorsal half and 9 exclusively the ventral half, and the remaining 11 spanned the midline of the myotome. The data are plotted as in Fig. 1*D* to show the innervation ranges of stage 42 MNs and compared with equivalent data from stage 37/38 (gray, *Left*). (*C*, *i*) Graph of soma sizes of stage 42 MNs versus spinal position labeled from all dorsoventral (1–0) locations. (*C*, *ii*) Backfill from ventral muscle with rhodamine dextran reveals somata occupying medial-ventral location. Stage 42 MNs have a more extensive dendritic field compared with stage 37/38 (19). (*C*, *iii*) Simultaneous backfill from ventral (rhodamine, red) and dorsal (FITC, green) muscle regions. Note nonoverlapping groups occupying similar dorsoventral region of cord.

Our stage 42 MN recordings support this hypothesis because they reveal considerable heterogeneity in firing properties during swimming (Fig. 4 *A*–*C*). Larval MNs with very low firing probabilities were generally active near the beginning of each swimming episode when rhythm frequency and intensity are at their highest (Fig. 4 *A*, *i*), but these neurons could also be recruited when the swimming rhythm accelerated (Fig. 4 *A*, *i* and *ii*). At the other end of the spectrum, some MNs were active essentially throughout entire episodes (Fig. 4 *C*, *i*) and, in this respect, resembled embryonic MNs. However, these lower-threshold MNs differed from embryonic ones in their ability to fire multiple impulses per cycle (Fig. 4 *C*, *ii*). In between were MNs that were active for a proportion of each swim episode (Figs. 2*E*, *i* and 4*B*, *i*). These neurons would periodically fall silent, but could be recruited during periods of acceleration. Are the differences in firing probability during swimming mirrored in the responses of MNs to injected depolarizing current steps? The spike thresholds (minimum injected current needed for inducing action potentials) broadly matched the recruitment order during swimming with higher-threshold neurons generally having lower-firing probabilities [Fig. 4*D*; gray scale depicts 100% probability (black) and 0% (white)]. We found

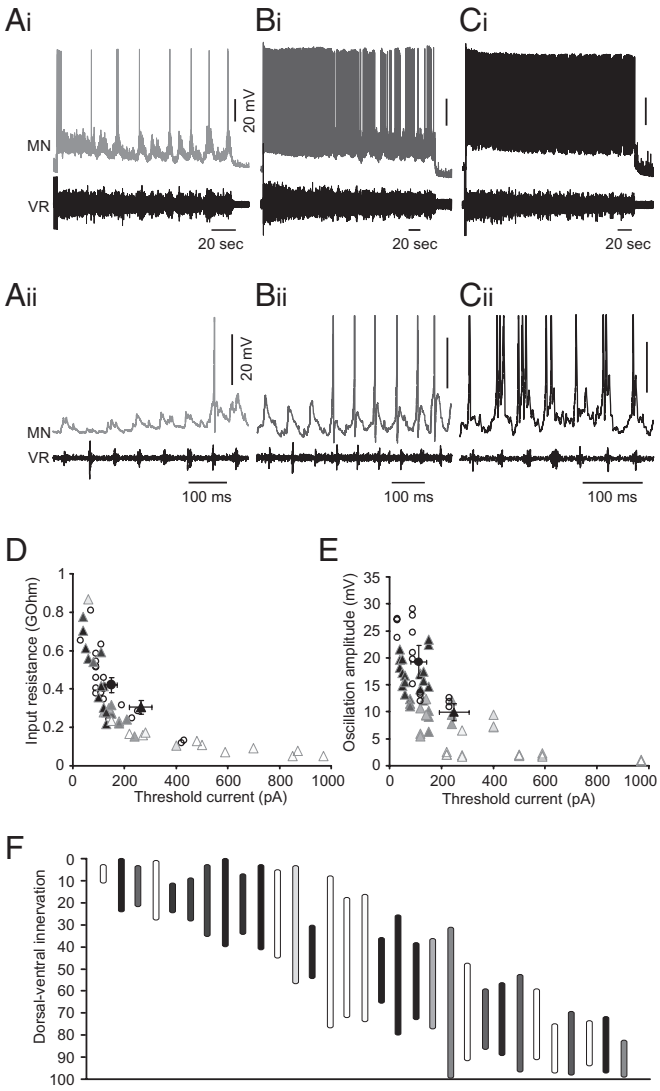

Fig. 4. Differentiation of larval MN electrical properties. Examples of stage 42 MNs with differing firing probabilities (the proportion of swim cycles in which the MN fired) during swimming: relatively low (*A*, light gray), medium (*B*, dark gray), and high (*C*, black). (*A*, *i*; *B*, *i*; and *C*, *i*) Whole episodes. (*A*, *ii*; *B*, *ii*; and *C*, *ii*) Expanded excerpts from same episodes. Action potentials in *A*, *ii*; *B*, *ii*; and *C*, *ii* have been truncated. (*D*) Plot of input resistance versus rheobase for stage 37/38 MNs (open circles; $n = 20$) and stage 42 MNs (gray triangles; $n = 34$). Gray scale for each stage 42 MN represents the percentage of cycles in which the MNs fired averaged over three episodes (black, 100%; white, 0%). Black circle and black triangle show means ± SE for the stage 37/38 and stage 42 MN groups, respectively. (*E*) Synaptic oscillation amplitudes of stage 42 MNs ($n = 18$; triangles using same gray scale) compared with stage 37/38 MNs ($n = 5$; circles). The amplitude is mean of 40–100 cycles near starts and ends of episodes. Black circle and black triangle show means ± SE for the stage 37/38 and stage 42 MN groups, respectively. (*F*) Innervation profiles for all stage 42 MNs recorded in gray scale according to the firing probability during swimming (cf. Fig. 3*B*). Note that each region of the myotome receives input from MNs across the range of firing probabilities.

a clear correlation between spike threshold and input resistance (Fig. 4*D*; $R^2 = 0.94$). Stage 42 MNs possessed a wider range of input resistance and threshold current and, on average, had significantly lower input resistances ($P < 0.05$) and higher rheobases ($P < 0.05$) than stage 37/38 MNs. The activation of MNs is based partly on their individual electrical properties, in addition to any frequency-dependent differences in the strength of the synaptic drive during fictive swimming, and the oscillation amplitude and rheobase of stage 42 MNs were broadly correlated (Fig. 4*E*; $R^2 = 0.68$). Stage 37/38 MNs received rhythmic synaptic drive of more consistent cycle-by-cycle amplitude, which was significantly higher than that of stage 42 MNs (Fig. 4*E*; $P < 0.001$), presumably ensuring that stage 37/38 MNs fire reliably.

Finally, is there a relationship between the innervation field of a MN and its position in the recruitment hierarchy during larval swimming? We compared the firing probabilities and innervation fields, but found no clear correlation. Indeed, when the innervation field data of Fig. 3*B* are replotted using the same gray scale as above [0% firing probability (white) and 100% (black)], it becomes clear that each dorsoventral region of the myotome is innervated by a mixture of MNs spanning the range of different firing probabilities. These results suggest that, by larval stage 42, a more refined control system for different regions of each myotome develops, allowing for the recruitment of progressively higher threshold MNs as swimming frequency and intensity increase.

Discussion

The vertebrate CNS contains a basic locomotor network from early stages of development, but the motor output often lacks flexibility. During postembryonic development, therefore, CPGs are modified to accommodate the changing behavioral requirements of later stages. In many model systems, rhythmic locomotor activity is drug-induced. Although this approach has greatly facilitated investigation of CPG networks, their neuromodulation, and their development (1–4), it also constrains the networks to operate over a relatively narrow range of possible output configurations, producing a single mode of operation dictated by the concentration and mixture of the drugs. This approach therefore precludes an appreciation of the complexity of naturally evoked and sustained motor network activity, which can operate like a rheostat over an almost infinitely wide range of frequencies and intensities. Two simpler model systems, the zebrafish and the *Xenopus* frog tadpole, generate fictive locomotion in the absence of drugs, which allows investigations of neuronal networks during near-normal operation and affords an opportunity to study how these networks emerge during development (3, 10, 13, 14). We focused on changes in MNs controlling the swimming behavior of postembryonic *Xenopus* frog tadpoles. In a brief 24-h period, MNs differentiate, both in firing properties and peripheral innervation fields, in a manner that promotes the control of movement direction and speed during 3D navigation through the environment. The possibility that new MNs differentiate between stages 37/38 and 42 can be rejected because the total number of MNs is relatively constant over this period of *Xenopus* development, and most have already differentiated by stage 22 (19). Numbers peak at stage 37/38 in rostral spinal cord regions at around 13/100 μm (20), similar to our data using fluorescent backfilling of MNs at both stage 37/38 and stage 42 (Fig. 3 *C*, *iii*).

We describe a rapid reconfiguration of the spinal motor pool that involves the retraction of some peripheral processes and the extension of others to transform MNs with broad dorsoventral innervation fields into ones that are more restricted to predominantly dorsal, medial, or ventral regions of the myotome. How does this developmental organization compare with other aquatic vertebrates? In zebrafish, the first MNs to reach the myotomes are the large primary MNs (of which there are only three to four per hemisegment) that selectively innervate dorsal, ventral, or lateral regions (21, 22). Secondary MNs are smaller and more numerous (around 20 per hemisegment), and they innervate the muscle block later, tracking along one of the three pathways pioneered by the primary MNs (22). In amphibians, the terms "primary" and "secondary" MN pools have been used by some authors to refer to those innervating the axial muscles and the limb muscles, respectively (reviewed in ref. 20). At stage 37/38 in *Xenopus* tadpoles, however, there is no anatomical evidence for segregation of axial MNs into two subgroups based on

soma size or position, as there is in zebrafish (21). It has been proposed that, by the early larval stages in *Xenopus*, a developing discontinuity in the distribution of MN soma diameters justifies separation into primary and secondary axial MN pools (23), as in teleosts (21, 24). Therefore, the MNs studied in the present paper, although "primary" using amphibian terminology, probably correspond to a mixture of both the larger primary and smaller secondary MN subtypes described in zebrafish (7, 21). If so, then it is of interest from an evolutionary perspective that the developmental program of axial MN differentiation in an amphibian like *Xenopus*, with initially broad innervation fields that are subsequently refined, differs significantly compared with fish, in which more refined innervation fields are specified from the outset.

At stage 37/38, *Xenopus* MNs form a near-continuous double row occupying approximately the ventral-most 25% of the cord, and they are morphologically homogenous (20, 27). There is little scope, therefore, at this earlier stage of development for the sort of dorsoventral MN recruitment map described for zebrafish. Do the dorsoventral innervation fields of stage 42 MNs parallel a dorsoventral distribution of somata in the spinal cord? Backfills using two fluorescent dyes revealed that the cell bodies are intermingled and occupy a similar dorsoventral region of the spinal cord. This suggests that, although there is no obvious dorsoventral spatial map in the spinal cord coding peripheral innervation, the innervation fields are indeed segregated into restricted areas of each muscle block. In addition, cell-body diameters spanned a relatively narrow range, ruling out the possibility that different regions of the myotome might be served by MNs with separate thresholds based exclusively on the size principle (25). An elegant recent study in zebrafish larvae on how neurons are recruited during different speeds of locomotion revealed a dorsoventral ordering of MNs (10), an organization that persists in the adult (26). Ventral MNs are active at low fictive swimming frequencies, and there is a progressive and orderly recruitment of more dorsal MNs as swim speed increases. A similar recruitment order exists for the excitatory interneurons that drive larval zebrafish swimming, but, interestingly, the opposite applies to the population of commissural inhibitory interneurons, with dorsal ones active at the lower frequencies. These authors showed that there is no particular correlation between soma size and recruitment order, seemingly at odds with Henneman's size principle (25), but input resistance and recruitment order are correlated, as we have also found.

We also show that the development of a more flexible larval swimming rhythm is not dependent on activity because it occurs apparently normally in animals that are developed under MS222 anesthesia (Fig. 2*D*). In normal development (and presumably also in the absence of activity), MNs become functionally differentiated such that, by stage 42, they (*i*) can fire multiple impulses in each cycle of swimming; (*ii*) may " drop out" of the rhythm as it slows down and weakens, but become available if swimming speeds up and intensifies; and (*iii*) form a more heterogeneous pool comprising members with distinct electrical properties and synaptic drive, similar to zebrafish (10, 26). This combination of changes provides the larval rhythm with increased flexibility because the intensity and frequency of rhythmic activation of the muscles can change dramatically on a cycle-by-cycle basis. Moreover, changes in the discharge on the left and right sides provide a mechanism for altering the direction of swimming in the left–right or yaw plane. The motor pool within one side has differentiated into a mixture of MNs with more restricted innervation fields (Fig. 3), providing the facility for differential control in the dorsoventral axis, which offers directional control in the pitch and roll planes. The fact that each sector of the myotome is contacted by MNs with different firing probabilities during swimming also provides a neural substrate for fine frequency control. We have not directly addressed how or when such changes are implemented behaviorally. However, accelerations in swimming frequency (28)—triggered, for example, by an extrinsic sensory input such as dimming the illumination (29)—causes the dorsal parts of the myotome to contract more than the ventral parts, in turn causing the body to arch upwards.

Motor system development involves a period of refinement of the synaptic connectivity and electrical properties of CPG neurons. In *Xenopus* tadpoles, this coincides with the prelude to a free-swimming, free-feeding larval existence in which adaptability of motor behavior is critical to survival. We have illuminated two key features of the myotomal MN pool that are prerequisite to the acquisition of flexible motor behavior, namely the differentiation of firing properties dictating recruitment order during swimming and the restriction of the peripheral innervation fields within the dorsoventral plane of each myotomal muscle block.

Methods

All experiments were performed on *X. laevis* tadpoles at either hatching stage 37/38 or larval stage 42 (15). Animals were obtained by hormone-assisted (CG injection; 1,000 U/mL; Sigma) matings of adults selected from an in-house breeding colony. Fertilized ova were collected and reared in enamel trays at 17–23 °C to stagger their development until they reached the desired stage. All experiments comply with UK Home Office regulations and have been approved by the University of St Andrews Animal Welfare Ethics Committee.

Electrophysiology. Tadpoles were briefly anesthetized with 0.1% MS-222 (3-aminobenzoic acid ester; Sigma), and the trunk skin was gashed to facilitate immobilization in 12.5 μM α-bungarotoxin (Sigma) saline; the tadpoles were then pinned in a bath of saline (in mM: 115 NaCl, 3 KCl, 2 $CaCl_2$, 2.4 $NaHCO_3$, 1 $MgCl_2$, 10 Hepes, adjusted with 4 M NaOH to pH 7.4). One or both sides of the trunk skin overlying the myotomal muscles were removed. Extracellular recordings of fictive swimming were made with suction electrodes from ventral roots at intermyotomal clefts. The dorsal parts of rostral myotomes were freed from the spinal cord, and the spinal cord was opened to the neurocoel for patch electrode access. Extracellular signals were amplified using differential AC amplifiers (A-M Systems model 1700), digitized using an Axon Digidata 1322A, and stored and processed on a PC computer using Axoscope v10. Simultaneous recordings were made from up to three ventral roots, normally located rostrally at the 4th and more caudally at the 11th or 12th postotic clefts on the left side and at the 6th to 8th cleft on the right side. Fictive swimming was initiated either by dimming the illumination or by stimulating through a glass suction electrode placed on the tail skin, which delivered a 1-ms current pulse via a DS2A isolated stimulator (Digitimer).

Whole-cell patch-clamp recordings in current clamp mode were made using electrodes pulled on either a Narishige PP830 or a Sutter P97 pipette puller from borosilicate glass capillaries (Harvard Apparatus Ltd.). All recordings were made from MNs at relatively rostral locations in the spinal cord, between the fourth and sixth postotic clefts. Patch pipettes were filled with 0.1% neurobiotin in the intracellular solution (in mM: 100 K-gluconate, 2 $MgCl_2$, 10 EGTA, 10 Hepes, 3 Na_2ATP, 0.5 NaGTP adjusted to pH 7.3 with KOH) and had resistances of ~10 MΩ. Recordings in whole-cell mode were amplified with an Axoclamp 2B amplifier and digitized using a CED power 1401. All signals were displayed and saved on a PC using Spike2 software. Neuronal anatomy was revealed as described previously (30).

Anatomy. MNs were back-filled using dextran-conjugated dyes (rodamine/FITC; Invitrogen). A thick paste, formed by mixing the powder with a small volume of distilled water, was loaded onto the tip of a sharp tungsten needle. Tadpoles were immobilized in MS222, as above. The saline was drained until the tadpole was beached on a Sylgard stage. The loaded pin was inserted through the skin on the left side and into the targeted muscle. The tadpole was refloated in saline and allowed to recover for 2 h and then reanesthetized and fixed in 4% paraformaldehyde overnight. Subsequently, preparations were rinsed in phosphate buffer saline and dissected to expose the spinal cord and then mounted in aqueous mounting medium (CC mount; Sigma) before being observed under a Leica confocal microscope and analyzed in ImageJ.

Anesthesia. To study the development of the locomotor system in the absence of movement, embryos were anesthetized in 0.015% MS222 (1:20 saline in distilled water, pH 7.4) either from stage 22 (before the onset of movement)

or from stage 37/38 until they had reached stage 42. The animals appeared to have developed completely normally. They were removed from the MS222 and immobilized, as before, in 12.5 μM α-bungarotoxin (Sigma) and prepared for ventral root recordings during fictive swimming.

Analysis. Electrophysiological data were analyzed using Dataview software (v 6.32, courtesy of W. J. Heitler, School of Biology, University of St Andrews, St Andrews, UK), and then all raw data were imported into Excel spreadsheets. Statistical analysis was performed in GraphPad (InStat v. 3.06) using unpaired *t* tests, with Welch correction applied as appropriate. Results are presented as mean ± SE, and differences are considered significant at $P < 0.05$.

ACKNOWLEDGMENTS. We thank Gareth Miles, Becka Bjornfors, Stephen Currie, and Nick Scott for helpful comments on the manuscript. This work was supported by project grants to K.S. from the Biotechnology and Biological Sciences Research Council and the Wellcome Trust to whom we are grateful.

1. Grillner S, Wallén P, Saitoh K, Kozlov A, Robertson B (2008) Neural bases of goal-directed locomotion in vertebrates: An overview. *Brain Res Brain Res Rev* 57:2–12.
2. Vinay L, Pearlstein E, Clarac F (2010) Development of spinal cord locomotor networks controlling limb movements. *Oxford Handbook of Developmental Behavioral Neuroscience*, eds Bumberh MS, Freeman JH, Robinson SR (Oxford University Press, New York), pp 210–239.
3. Sillar KT (2010) Development of spinal motor networks controlling axial movements. *Oxford Handbook of Developmental Behavioral Neuroscience*, eds Bumberg MS, Freeman JH, Robinson SR (Oxford University Press, New York), pp 240–253.
4. Grillner S, Jessell TM (2009) Measured motion: Searching for simplicity in spinal locomotor networks. *Curr Opin Neurobiol* 19:572–586.
5. Dasen JS, Jessell TM (2009) Hox networks and the origins of motor neuron diversity. *Curr Top Dev Biol* 88:169–200.
6. Jessell TM (2000) Neuronal specification in the spinal cord: Inductive signals and transcriptional codes. *Nat Rev Genet* 1:20–29.
7. Eisen JS (1999) Patterning motoneurons in the vertebrate nervous system. *Trends Neurosci* 22:321–326.
8. Spitzer NC (2006) Electrical activity in early neuronal development. *Nature* 444: 707–712.
9. Hanson MG, Landmesser LT (2006) Increasing the frequency of spontaneous rhythmic activity disrupts pool-specific axon fasciculation and pathfinding of embryonic spinal motoneurons. *J Neurosci* 26:12769–12780.
10. McLean DL, Fan J, Higashijima S, Hale ME, Fetcho JR (2007) A topographic map of recruitment in spinal cord. *Nature* 446:71–75.
11. Bhatt DH, McLean DL, Hale ME, Fetcho JR (2007) Grading movement strength by changes in firing intensity versus recruitment of spinal interneurons. *Neuron* 53:91–102.
12. Wallén P, Grillner S, Feldman JL, Bergelt S (1985) Dorsal and ventral myotome motoneurons and their input during fictive locomotion in lamprey. *J Neurosci* 5:654–661.
13. Roberts A, Li W-C, Soffe SR (2010) How neurons generate behavior in a hatchling amphibian tadpole: An outline. *Front Behav Neurosci* 4:16.
14. Sillar KT, Wedderburn JFS, Simmers AJ (1991) The postembryonic development of locomotor rhythmicity in *Xenopus* laevis tadpoles. *Proc R Soc Lond B Biol Sci* 246:147–153.
15. Nieuwkoop PD, Faber J (1956) *Normal Tables of Xenopus laevis (Daudin)* (North Holland, Amsterdam).
16. Roberts A, Kahn JA, Soffe SR, Clarke JDW (1981) Neural control of swimming in a vertebrate. *Science* 213:1032–1034.
17. Sillar KT, Roberts A (1993) Control of frequency during swimming in *Xenopus* embryos: A study on interneuronal recruitment in a spinal rhythm generator. *J Physiol* 472:557–572.
18. Zhang H-Y, Li W, Heitler WJ, Sillar KT (2009) Electrical coupling synchronises spinal motorneuron activity during swimming in hatchling *Xenopus* tadpoles. *J Physiol* 587:4455–4466.
19. van Mier P, Armstrong J, Roberts A (1989) Development of early swimming in *Xenopus laevis* embryos: Myotomal musculature, its innervation and activation. *Neuroscience* 32:113–126.
20. Roberts A, Walford A, Soffe SR, Yoshida M (1999) Motoneurons of the axial swimming muscles in hatchling *Xenopus* tadpoles: Features, distribution, and central synapses. *J Comp Neurol* 411:472–486.
21. Westerfield M, McMurray JV, Eisen JS (1986) Identified motoneurons and their innervation of axial muscles in the zebrafish. *J Neurosci* 6:2267–2277.
22. Myers PZ, Eisen JS, Westerfield M (1986) Development and axonal outgrowth of identified motoneurons in the zebrafish. *J Neurosci* 6:2278–2289.
23. Nordlander RH (1986) Motoneurons of the tail of young *Xenopus* tadpoles. *J Comp Neurol* 253:403–413.
24. Fetcho JR (1987) A review of the organization and evolution of motoneurons innervating the axial musculature of vertebrates. *Brain Res* 434:243–280.
25. Henneman E, Clamann HP, Gillies JD, Skinner RD (1974) Rank order of motoneurons within a pool: Law of combination. *J Neurophysiol* 37:1338–1349.
26. Gabriel JP, et al. (2011) Principles governing recruitment of motoneurons during swimming in zebrafish. *Nat Neurosci* 14:93–99.
27. Roberts A, Clarke JDW (1982) The neuroanatomy of an amphibian embryo spinal cord. *Philos Trans R Soc Lond B Biol Sci* 296:195–212.
28. Jamieson D, Roberts A (2000) Responses of young *Xenopus laevis* tadpoles to light dimming: Possible roles for the pineal eye. *J Exp Biol* 203:1857–1867.
29. Foster RG, Roberts A (1982) The pineal eye in *Xenopus laevis* embryos and larvae: A photoreceptor with a direct excitatory effect on behaviour. *J Comp Physiol* 145: 413–419.
30. Li W-C, Soffe SR, Roberts A (2002) Spinal inhibitory neurons that modulate cutaneous sensory pathways during locomotion in a simple vertebrate. *J Neurosci* 22:10924–10934.